

See discussions, stats, and author profiles for this publication at: <https://www.researchgate.net/publication/261731386>

# Pushing the Theoretical Limit of Li-CFx Batteries: A Tale of Bifunctional Electrolyte

ARTICLE in JOURNAL OF THE AMERICAN CHEMICAL SOCIETY · APRIL 2014

Impact Factor: 12.11 · DOI: 10.1021/ja5026358 · Source: PubMed

CITATIONS

9

READS

116

## 5 AUTHORS, INCLUDING:



[Ezhiylmurugan Rangasamy](#)

Oak Ridge National Laboratory

23 PUBLICATIONS 318 CITATIONS

SEE PROFILE



[Juchuan \(JC\) Li](#)

Lawrence Berkeley National Laboratory

31 PUBLICATIONS 429 CITATIONS

SEE PROFILE



[Gayatri Sahu](#)

Oak Ridge National Laboratory

12 PUBLICATIONS 88 CITATIONS

SEE PROFILE



[Nancy J Dudney](#)

Oak Ridge National Laboratory

191 PUBLICATIONS 5,337 CITATIONS

SEE PROFILE

# Pushing the Theoretical Limit of Li-CF<sub>x</sub> Batteries: A Tale of Bifunctional Electrolyte

Ezhiylmurugan Rangasamy,<sup>†</sup> Juchuan Li,<sup>‡</sup> Gayatri Sahu,<sup>†</sup> Nancy Dudney,<sup>‡</sup> and Chengdu Liang<sup>\*,†</sup>

<sup>†</sup>Center for Nanophase Materials Sciences and <sup>‡</sup>Materials Sciences and Technology Division, Oak Ridge National Laboratory, Oak Ridge, Tennessee 37831, United States

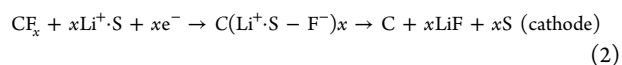
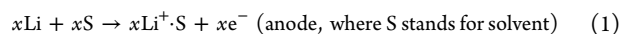
## S Supporting Information

**ABSTRACT:** In a typical battery, the inert electrolyte functions solely as the ionic conductor without contribution to the cell capacity. Here we demonstrate that the most energy-dense Li-CF<sub>x</sub> battery delivers a capacity exceeding the theoretical maximum of CF<sub>x</sub> with a solid electrolyte of Li<sub>3</sub>PS<sub>4</sub> (LPS) that has dual functions: as the inert electrolyte at the anode and the active component at the cathode. Such a bifunctional electrolyte reconciles both inert and active characteristics through a synergistic discharge mechanism of CF<sub>x</sub> and LPS. The synergy at the cathode is through LiF, the discharge product of CF<sub>x</sub>, which activates the electrochemical discharge of LPS at a close electrochemical potential of CF<sub>x</sub>. Therefore, the solid-state Li-CF<sub>x</sub> batteries output 126.6% energy beyond their theoretic limits without compromising the stability of the cell voltage. The additional energy comes from the electrochemical discharge of LPS, the inert electrolyte. This bifunctional electrolyte revolutionizes the concept of conventional batteries and opens a new avenue for the design of batteries with unprecedented energy density.

Artificial cardiac pacemakers, radiofrequency identification devices (RFID), remote keyless systems, and similar stand-alone devices represent a large demand for long-standing, high capacity batteries. Primary Li batteries cater to these applications and complement the secondary Li-ion batteries when the recharge of batteries is prohibited or not needed.<sup>1,2</sup> In a typical battery, the individual components such as electrodes, electrolyte, etc., have their functions preset and do not overlap with one another. However, the expendable nature of primary batteries paves way for a bifunctional design maneuver with the electrolyte, enabling it to function as the electrolyte and also as an electrode. A bifunctional electrolyte can greatly improve the capacity of primary batteries. Such a design places direct conflict on the electrolyte that even while becoming electrochemically active, it should remain stable with the other electrode at all times for the purpose of cell stability. Therefore, the activity of the bifunctional electrolyte should be localized at one electrode. It is essential that this activity is catalyzed and not spontaneous. The best scenario for such a design is that the electrochemical activity in the electrolyte is promoted by the product of discharge (cathode); therefore no additional catalyst is needed. Hence the ideal bifunctional electrolyte for lithium batteries should possess good ionic conductivity and be

inherently stable with metallic Li anode and electrochemically activated by the cathodic product of discharge.

The concept of a bifunctional electrolyte will be in stark contrast to the SOCl<sub>2</sub> catholytes utilized in the Li-SOCl<sub>2</sub> batteries where the electrolyte is the cathode that is active at all potentials and relies on a LiCl passive film to maintain stability with the anode.<sup>3</sup> The Li-CF<sub>x</sub> battery system offers one of the best energy densities with up to 7 times the capacity of LiCoO<sub>2</sub>-based Li-ion system, a conventional Li-ion battery cathode, and up to 2 times the capacity of thionyl chloride, the nearest energy dense primary cathode.<sup>4</sup> Additionally, the Li-CF<sub>x</sub> system is extremely stable, offering excellent shelf life (>10 years) and minimal (<10%) self-discharge.<sup>1,2</sup> To achieve even better performance of the best battery system, the concept of the bifunctional electrolyte has been implemented in the Li-CF<sub>x</sub> batteries. A conventional Li-CF<sub>x</sub> battery uses an inert liquid electrolyte. The solvation process is an indispensable part of the electrochemical reactions that are described by the following equations:<sup>5–7</sup>



Limitations of this battery chemistry, such as (1) heat generation during the course of reaction, (2) volume expansion resulting from the crystallization and precipitation of LiF, (3) poor electrode kinetics and low electronic conductivity restricting the performance at high discharge rates, and (4) flammability concerns with organic electrolytes, have restricted the widespread application of Li-CF<sub>x</sub> cells.<sup>5,8–14</sup> These limitations are closely linked to the solvation process of Li-CF<sub>x</sub> batteries. The volume expansion of the cathode could result from the intercalation of solvent into the carbon during discharge coupled with the voids pillared by the LiF crystallization between graphene layers, following discharge. The high enthalpy of crystallization for LiF (26.91 kJ mol<sup>−1</sup>)<sup>15</sup> results in heat generation during the discharge reaction.<sup>5</sup> A move away from the solvation chemistry would eliminate the volume expansion from solvent intercalation and result in the formation of amorphous LiF, minimizing the heat generation. Thus, the elimination of solvents is expected to be a fundamental improvement in current generation Li-CF<sub>x</sub> batteries. Solid-state Li-ion conductors offer a step away from the solvation chemistry while offering better mechanical

Received: March 19, 2014

Published: April 14, 2014



properties, electrochemical, and thermal stability.<sup>16–18</sup> Nanoporous  $\beta$ - $\text{Li}_3\text{PS}_4$  (LPS) has been recently reported as an excellent solid electrolyte that is stable with metallic lithium anode.<sup>19</sup> The multiple stable oxidation states (3+, 4+, and 5+) of P coupled with its 5+ oxidation state in LPS makes it an appealing candidate for a bifunctional electrolyte. We report herein LPS as a bifunctional solid electrolyte for  $\text{Li}-\text{CF}_x$  cells that deliver unprecedented capacity, far exceeding the theoretical values for  $\text{CF}_x$  cathodes.

LPS functions as an electrolyte with low interfacial resistance. As shown in Figure 1, the solid-state  $\text{Li}/\text{LPS}/\text{CF}_x$  cells exhibit a

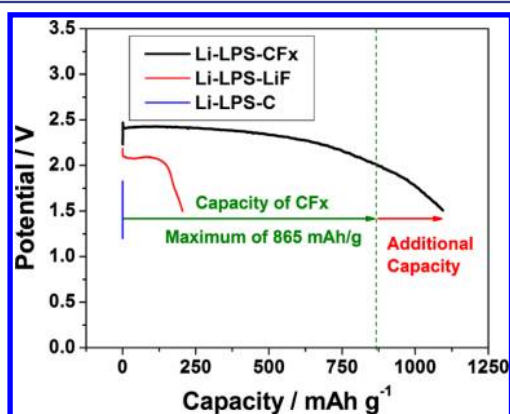


**Figure 1.** Discharge profile for the  $\text{Li}/\text{LPS}/\text{CF}_x+\text{C}+\text{LPS}$  cell at a rate of  $\text{C}/170$  and a current density of  $5 \mu\text{A g}^{-1}$  illustrates cell capacity exceeding the theoretical maximum of  $865 \text{ mAh g}^{-1}$  for the  $\text{CF}_x$  system. Discharge profiles for the  $\text{Li}/\text{LPS}/\text{C}+\text{LPS}$  and  $\text{Li}/\text{LPS}/\text{C}+\text{LiF}+\text{LPS}$  control cells at a current density of  $5 \mu\text{A g}^{-1}$  are also provided.

stable potential profile with capacity utilization of  $1095 \text{ mAh g}^{-1}$ , that exceeds the  $865 \text{ mAh/g}$  theoretical capacity<sup>12,13</sup> for the  $\text{CF}_x$  cathode (when  $x = 1$ ). The stability in potential is remarkable and is characteristic of the  $\text{Li}-\text{CF}_x$  system as observed in the earlier reports with wet cells.<sup>1,5,7–14,20</sup> The solid-state  $\text{Li}-\text{CF}_x$  cell exhibits an extremely low voltage delay of  $\approx 15 \text{ mV}$  in contrast to conventional liquid cells that typically exhibit a significant voltage delay of  $\sim 100 \text{ mV}$  resulting from the low electronic conductivity of  $\text{CF}_x$  when  $x \geq 0.9$ .<sup>9,13</sup> Such an unusually low voltage delay of the  $\text{CF}_x$  cathode is attributed to the good interfacial kinetics with LPS (as illustrated by EIS spectra in Figure S1) and excellent electronic conductivity from the C black. In fact, the interface resistance extracted from the EIS is less than half of the resistance attributed to the bulk electrolyte.

Activated discharge of LPS at the cathode: a demonstrated synergy of LPS and  $\text{CF}_x$ . A  $\text{Li}-\text{CF}_1$  cell delivering a capacity higher than the theoretical maximum of  $865 \text{ mAh g}^{-1}$  is unprecedented. Among the three components of the cathode:  $\text{CF}_x$ , carbon, and LPS, carbon is inert, while  $\text{CF}_x$  is theoretically limited. Therefore, the extra capacity must be attributed to the discharge of LPS, which is contradictory to its  $5 \text{ V}$  electrochemical window in literature.<sup>19</sup> A control experiment of  $\text{Li}/\text{LPS}/\text{C}$  cell without the use of  $\text{CF}_x$  in Figure 1 proved that LPS and carbon did not exhibit any meaningful capacity even when the current density was reduced to  $1.5 \mu\text{A cm}^{-2}$  (see Figure 1). In other words, LPS fulfils the role of an excellent electrolyte, which conducts lithium ions without electrochemical activity. The origin of the extra capacity was unveiled, while the second control cell of  $\text{Li}/\text{LPS}/\text{C}+\text{LiF}$  was tested under identical conditions (see Figure 1). When an inert

component of  $\text{LiF}$  was added to the cathode, the  $\text{LiF} + \text{C}$  cell exhibited a capacity in excess of  $200 \text{ mAh g}^{-1}$  (based on the mass of the cathode) with a stable cell voltage of  $2.1 \text{ V}$ . The capacity in the second control cell cannot come from  $\text{LiF}$  (as it cannot be further reduced) or C (which is electrochemically inactive at the observed potentials). This experiment manifests that  $\text{LiF}$  activates the electrochemical discharge of LPS. The discharge function is likely attributed to the electrochemical reduction of  $\text{P}^{5+}$  to lower oxidation states. It is known that the  $\text{P}^{5+}$  charge centers of  $(\text{PS}_4)^{3-}$  can be reduced to  $\text{P}^{4+}$  charge centers of  $(\text{P}_2\text{S}_6)^{4-}$ .<sup>21,22</sup> Thus, a transition from  $\text{Li}_3\text{PS}_4$  to  $\text{Li}_4\text{P}_2\text{S}_6$  is possibly triggered in the presence of  $\text{LiF}$ . However, the chemical compositions of the discharge mixture of LPS with  $\text{CF}_x$  need dedicated investigations because of the complex nature of discharge mixture and the high air sensitivity for the electrolyte.<sup>23</sup> Detailed mechanism of  $\text{LiF}$  activated discharge of LPS is currently underway.

This leads to a conclusion that  $\text{LiF}$  catalyzes an electrochemical activity in LPS that offers the additional capacity.  $\text{LiF}$  is a discharge product of  $\text{CF}_x$  at the potential of  $\sim 2.5 \text{ V}$ ; thereby a synergistic relationship is now formed between  $\text{CF}_x$  and LPS. As a discharge product of  $\text{CF}_x$ ,  $\text{LiF}$  is localized at the cathode. Therefore, at the anode side, LPS remains inert and functions solely as the electrolyte. At the cathode side, the synergistic interaction of  $\text{CF}_x$  and LPS confers a dual function to LPS: this electrolyte first functions as the  $\text{Li}$ -ion conductor that enables the discharge of  $\text{CF}_x$  to  $\text{LiF}$  at  $\sim 2.5 \text{ V}$  and in return the  $\text{LiF}$  activates the electrochemical discharge of LPS at  $2.1 \text{ V}$  which functions as an active component of the cathode. The synergistic relationship between  $\text{CF}_x$  and LPS is critical in converting an electrolyte that is conventionally an inactive component in capacity to an active one.

As stated earlier, primary batteries have a necessary requirement for long shelf life. Hence in such a synergistic relationship, it is necessary to ensure that this activity is unspontaneous. A sample of  $\text{LiF}/\text{LPS}$  mixture was high-energy ball milled and allowed to sit under ambient conditions to investigate the possibility of a spontaneous chemical reaction between the two phases. The XRD pattern of the  $\text{LiF}/\text{LPS}$  mixture showed no change even after 30 days. The results of this study (Figure S2) confirmed that the  $\text{LiF}/\text{LPS}$  mixture is electrochemically active instead of chemically reactive.

Solid-state cells offer new reaction chemistry to the  $\text{Li}-\text{CF}_x$  system. In a conventional  $\text{Li}-\text{CF}_x$  cell, the solvation process in the liquid electrolytes causes volume expansion, heat generation, and safety concerns. The absence of a solvent will thus significantly change the electrochemical pathway. XRD analysis (Figure 2a) of the pellets before and after discharge shows practically no change in crystallographic phases, more importantly does not reveal new phases. The observation of electrochemical capacity clearly suggests a phase change occurring within the cathode. An XPS analysis (Figure 2b) of the cycled cathode surface reveals the presence of  $\text{LiF}$ . The measured binding energy of  $685.54 \text{ eV}$  for F 1s is in line with the earlier reports for  $\text{LiF}$ <sup>24–26</sup> and with the measured binding energy of  $685.4 \text{ eV}$  for a  $\text{LiF}$  standard obtained from Sigma-Aldrich. XRD is an effective representation of crystallographic phases within a system. The lack of concrete evidence for  $\text{LiF}$  in the XRD data and the presence of  $\text{LiF}$  in XPS clearly suggest that the discharge formed amorphous  $\text{LiF}$ . Upon close examination of XRD, minor evidence of an amorphous phase is observed between  $36^\circ$  and  $48^\circ$  that corresponds to the crystallographic reflections of  $\text{LiF}$  (highlighted regions in Figure

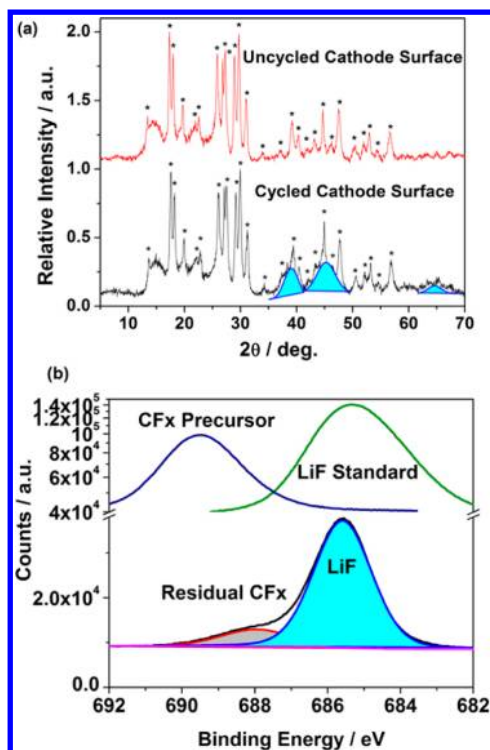
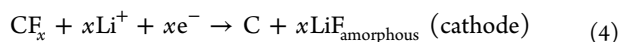
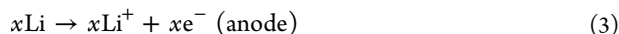


**Figure 2.** (a) XRD data for the cathode surface before and after cycling. The peaks corresponding to  $\beta$ - $\text{Li}_3\text{PS}_4$  have been indexed with \*. (b) XPS analysis of the cathode surface illustrates the formation of LiF along with trace CF thus indicating that the LiF is indeed amorphous.

2a). This provides further evidence for amorphous LiF. Since no solvation occurs in a solid-state Li-ion conductor, the reaction pathway for an all solid  $\text{Li}-\text{CF}_x$  cell can be elucidated as



The transition from solvation chemistry to solid-state chemistry has taken place under LPS without any performance setbacks. Additionally, amorphous LiF sidesteps the enthalpy of crystallization resulting in the absence of any measurable heat generated.

However, the formation of a new phase will always result in volumetric changes, because of the varying densities.<sup>15</sup> The favorable elastic modulus of the solid-state electrolytes could be utilized to resist volume expansion.<sup>16</sup> A 3D network encompassing C,  $\text{CF}_x$ , and LPS will hence aid in mitigating the residual volumetric concerns while providing a favorable conducting framework. This framework is obtained by utilizing an hour long milling procedure between the  $\text{CF}_x$  cathode and C-black and subsequent milling of the mixture with the soft LPS (Figure S3). An elemental map of the electrode surface reveals a homogeneous distribution of S and P (LPS) within a C and F matrix ( $\text{CF}_x + \text{C}$ ). Typical solid-state mixing procedures result in inhomogeneities and agglomerations, however the mechanical properties of C and  $\text{CF}_x$  aid in obtaining good dispersion even under dry milling conditions. As a result, this 3D interconnected architecture provides a framework within the cathode composite that mitigates volume expansion. This is clearly observed under the SEM (Figure 3) where an uncycled cathode has a pristine electrode surface

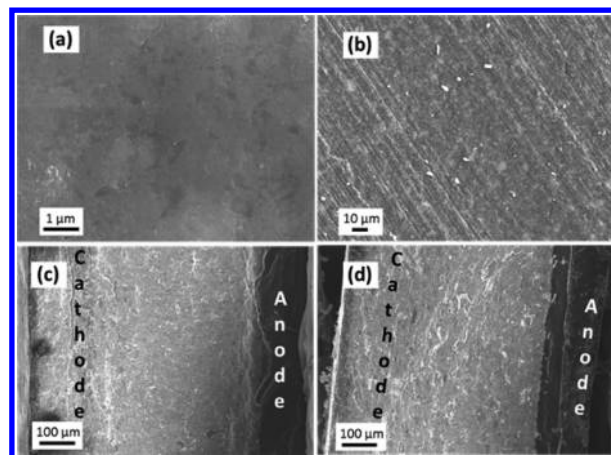


**Figure 3.** SEM images of  $\text{Li}-\text{CF}_x$  cells (a) before and (b) after C/30 electrochemical discharge at ambient temperature and  $65^\circ\text{C}$ . Cross-sectional images of  $\text{Li}/\text{LPS}/\text{CF}_x$  cell (c) after and (d) before cycling at ambient temperature. Thickness of the cell was measured at  $878.7\ \mu\text{m}$  prior to cycling and  $878.1\ \mu\text{m}$  after cycling.

(Figure 3a), while the cycled cells show micrometer and submicrometer level textural changes (Figure S4). However, these changes are not observed at lower magnifications (Figure 3b), thus indicating that the integrity of the electrode is always preserved.

Micron level textural changes are the mechanism for accommodating small volume changes within the cathode and are unavoidable due to the nature of the reaction. Cross sectional SEM imaging (Figure 3c,d) of the cells prior and subsequent to cycling reveal the absence of macroscopic volumetric change on the cells. Due to the minimal volume change, 3D interconnected network remains unaffected during the course of cell discharge. The formation of amorphous LiF coupled with the lack of significant volume change, thereby offers additional evidence that the crystallization of LiF is primarily the cause for volumetric changes observed in liquid  $\text{Li}-\text{CF}_x$  cells.

Solid-state  $\text{Li}-\text{CF}_x$  cells deliver good rate performance. While primary batteries are not typically subjected to high rate conditions, they do require moderate rate performance for certain applications. The solid state  $\text{Li}-\text{CF}_x$  cells clearly show excellent rate performance, with the cells delivering higher than theoretical capacities and very minimal polarization. Solid-state electrolytes follow an Arrhenius-type behavior, thus exhibiting better transport properties at elevated temperatures.<sup>16,18</sup> In order to demonstrate their high temperature performance,  $\text{Li}-\text{CF}_x$  cells were cycled at ambient temperature and  $65^\circ\text{C}$ . As can be evidenced by the comparative data (Figure 4), the heated solid-state cells deliver better performance with higher than theoretical capacities under rates as high as C/30. This can be attributed to two factors: (1) improvement in the Li-ion conductivity for the LPS electrolyte and (2) better interfacial kinetics resulting in much lower polarization losses. This is evident from the difference in operating potential between the cells discharged at ambient conditions and at elevated temperatures.

The results presented in this study demonstrate a bifunctional utility of LPS electrolyte within the  $\text{Li}-\text{CF}_x$  primary system. This electrochemical activity of LPS is triggered by LiF resulting in a tandem discharge of  $\text{CF}_x$  and LPS through cooperative interactions of the electrolyte and electrode. As



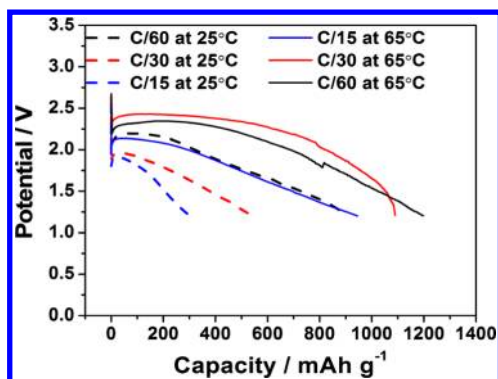


**Figure 4.** Rate performance of the Li-CF<sub>x</sub> cells is illustrated at ambient conditions and at 65 °C. It is clearly evident that the solid-state cells deliver an excellent rate performance as required for primary cells.

necessitated by design, the electrolyte maintains its stability with the Li anode at all times. The solid-state Li-CF<sub>x</sub> cells exhibit excellent capacity and good rate performance. The application of a solid electrolyte has resulted in a new nonsolvated electrochemical pathway for the Li-CF<sub>x</sub> system. The formation of amorphous LiF coupled with the mitigated volume expansion and heat generation provides concrete evidence that the solid-state Li-CF<sub>x</sub> system exceeds the conventional liquid cell in all aspects. Currently studies are underway to examine and clearly elucidate a reaction mechanism for the capacity offered by LPS. It can be concluded that the concept of bifunctional electrolyte is a significant path forward for batteries with energy density pushing their theoretical maxima in a conventional setup.

## ■ ASSOCIATED CONTENT

### ● Supporting Information

Experimental details and additional data. This material is available free of charge via the Internet at <http://pubs.acs.org>.

## ■ AUTHOR INFORMATION

### Corresponding Author

liangcn@ornl.gov

### Notes

The authors declare no competing financial interest.

## ■ ACKNOWLEDGMENTS

This work was sponsored by the U.S. Department of Energy (DOE), Office of Basic Energy Sciences, Division of Materials Sciences and Engineering. The synthesis and characterization of materials were conducted at the Center for Nanophase Materials Sciences, which is sponsored at Oak Ridge National Laboratory by the Division of Scientific User Facilities, U.S. DOE.

## ■ REFERENCES

- (1) Greatbatch, W.; Holmes, C. F.; Takeuchi, E. S.; Ebel, S. J. *Pace* **1996**, *19*, 1836.
- (2) Vincent, C. A. *Solid State Ionics* **2000**, *134*, 159.
- (3) Schlaikjer, C. R.; Goebel, F.; Marincic, N. J. *Electrochem. Soc.* **1979**, *126*, 513.
- (4) *Lithium Batteries*; Nazri, G. A.; Pistoia, G., Eds.; Springer: New York, 2003.
- (5) Zhang, S. S.; Foster, D.; Wolfenstine, J.; Read, J. J. *Power Sources* **2009**, *187*, 233.
- (6) Whittingham, M. S. J. *Electrochem. Soc.* **1975**, *122*, 526.

- (7) Watanabe, N. *Solid State Ionics* **1980**, *1*, 87.
- (8) Meduri, P.; Chen, H. H.; Xiao, J.; Martinez, J. J.; Carlson, T.; Zhang, J. G.; Deng, Z. D. *J. Mater. Chem. A* **2013**, *1*, 7866.
- (9) Zhang, Q.; D'Astorg, S.; Xiao, P.; Zhang, X.; Lu, L. *J. Power Sources* **2010**, *195*, 2914.
- (10) Zhang, S. S.; Foster, D.; Read, J. J. *Power Sources* **2009**, *188*, 601.
- (11) Zhang, S. S.; Foster, D.; Read, J. J. *Power Sources* **2009**, *188*, 532.
- (12) Nagasubramanian, G.; Sanchez, B. J. *Power Sources* **2007**, *165*, 630.
- (13) Lam, P.; Yazami, R. *Power Sources* **2006**, *153*, 354.
- (14) Hany, P.; Yazami, R.; Hamwi, A. *J. Power Sources* **1997**, *68*, 708.
- (15) Haynes, W. M. *CRC Handbook of Chemistry and Physics*, 93rd ed.; Taylor & Francis: Boca Raton, FL, 2012.
- (16) Knauth, P. *Solid State Ionics* **2009**, *180*, 911.
- (17) Cho, Y. H.; Wolfenstine, J.; Rangasamy, E.; Kim, H.; Choe, H.; Sakamoto, J. *J. Mater. Sci.* **2012**, *47*, 5970.
- (18) Takada, K. *Acta Mater.* **2013**, *61*, 759.
- (19) Liu, Z.; Fu, W.; Payzant, E. A.; Yu, X.; Wu, Z.; Dudney, N. J.; Kiggans, J.; Hong, K.; Rondinone, A. J.; Liang, C. *J. Am. Chem. Soc.* **2013**, *135*, 975.
- (20) Yazami, R.; Hamwi, A.; Guerin, K.; Ozawa, Y.; Dubois, M.; Giraudet, J.; Masin, F. *Electrochem. Commun.* **2007**, *9*, 1850.
- (21) Evenson, D.; Dorhout, P. K. *Inorg. Chem.* **2001**, *40*, 2884.
- (22) Tachez, M.; Malugani, J. P.; Mercier, R.; Robert, G. *Solid State Ionics* **1984**, *14*, 181.
- (23) The cycled surfaces and pellets have been subjected to multiple characterization techniques such as Raman, XPS, and XRD. However the absence of significant crystallographic phase changes the presence of signal absorbing C, and multiple phases have prevented the identification of oxidation state changes within the LPS.
- (24) Edstrom, K.; Herstedt, M.; Abraham, D. P. *J. Power Sources* **2006**, *153*, 380.
- (25) Eshkenazi, V.; Peled, E.; Burstein, L.; Golodnitsky, D. *Solid State Ionics* **2004**, *170*, 83.
- (26) Ismail, I.; Noda, A.; Nishimoto, A.; Watanabe, M. *Electrochim. Acta* **2001**, *46*, 1595.